HHS Public Access

Author manuscript

Dev Biol. Author manuscript; available in PMC 2018 September 01.

Published in final edited form as:

Dev Biol. 2017 September 01; 429(1): 147–157. doi:10.1016/j.ydbio.2017.06.035.

PKA-mediated Gli2 and Gli3 phosphorylation is inhibited by Hedgehog signaling in cilia and reduced in Talpid3 mutant

Jia Li[a,b,1,2], **Chengbing Wang**[b,1], **Chuanqing Wu**[b,d,3], **Ting Cao**[b,e,4], **Guoqiang Xu**[f], **Qing Meng**[a,*], and **Baolin Wang**[b,c,*,**]

[a]Institute of Biological Sciences and Biotechnology, Donghua University, Shanghai 201620, China

[b]Department of Genetic Medicine, Weill Medical College of Cornell University, 1300 York Avenue, W404, New York, NY 10065, USA

[c]Department of Cell and Developmental Biology, Weill Medical College of Cornell University, 1300 York Avenue, W404, New York, NY 10065, USA

[d]Department of Gastrointestinal Surgery, Union Hospital, Tongji Medical College, Huazhong University of Science and Technology, Wuhan 430030, Hubei, China

[e]College of Pharmaceutical Sciences, Soochow University, Suzhou, Jiangsu, China

[f]Jiangsu Key Laboratory of Translational Research and Therapy for Neuro-Psycho-Diseases and College of Pharmaceutical Sciences, Jiangsu Key Laboratory of Preventive and Translational Medicine for Geriatric Diseases, Soochow University, Suzhou, Jiangsu, China

Abstract

Hedgehog (Hh) signaling is thought to occur in primary cilia, but the molecular basis of Gli2 and Gli3 activation by Hh signaling in cilia is unknown. Similarly, how ciliary gene mutations result in reduced Gli3 processing that generates a repressor is also not clear. Here we show that Hh signaling inhibits Gli2 and Gli3 phosphorylation by protein kinase A (PKA) in cilia. The cilia related gene *Talpid3* (*Ta3*) mutation results in the reduced processing and phosphorylation of Gli2 and Gli3. Interestingly, Ta3 interacts and colocalizes with PKA regulatory subunit PKARIIβ at centrioles in the cell. The centriolar localization and PKA binding regions are located in the N- and C-terminal regions of Ta3, respectively. PKARIIβ fails to localize at centrioles in some *Ta3* mutant cells. Therefore, our study provides the direct evidence that Gli2 and Gli3 are dephosphorylated and activated in cilia and that impaired Gli2 and Gli3 processing in *Ta3* mutant is at least in part due to a decrease in Gli2 and Gli3 phosphorylation.

[*]Corresponding author. mengqing@dhu.edu.cn (Q. Meng). [**]Corresponding author at: Department of Genetic Medicine, Weill Medical College of Cornell University, 1300 York Avenue, W404, New York, NY 10065, USA. baw2001@med.cornell.edu (B. Wang).
[1]These authors contributed equally.
[2]Current address: Institute of Biological Sciences and Biotechnology, Donghua University, China.
[3]Current address: Department of Gastrointestinal Surgery, Union Hospital, Tongji Medical College, Huazhong University of Science and Technology, China.
[4]Current address: College of Pharmaceutical Sciences, Soochow University, China.

Appendix A. Supporting information

Supplementary data associated with this article can be found in the online version at http://dx.doi.org/10.1016/j.ydbio.2017.06.012.

Keywords

Hedgehog; Gli2; Gli3; Talpid3; PKA; Cilia

1. Introduction

The Hedgehog (Hh) family of secreted signaling proteins plays fundamental roles in cell fate specification, proliferation, and differentiation. Loss of Hh signaling results in a wide range of birth defects, whereas aberrant activation of the Hh pathway causes several types of human cancer (Jiang and Hui, 2008). Hh signaling is initiated by the binding of Hh to its receptor Patched (Ptch) (Fuse et al., 1999; Stone et al., 1996), a twelve-pass membrane protein, followed by releasing Ptch inhibition to Smoothened (Smo), a G-protein coupled receptor (GPCR) (Riobo et al., 2006). In vertebrates, Smo then transduces signals downstream and ultimately actives the Gli2 and Gli3 zinc-finger-containing transcription factors, which in turn upregulate the expression of Hh targets, including *Ptch1* and *Gli1*, another member of the Gli family (Goodrich et al., 1996; Marigo et al., 1996). Gli2 acts primarily as a transcriptional activator, whereas Gli3 largely serves as a repressor, though it also functions as a weak activator (Bai et al., 2004). Consistent with their functions, our previous studies showed that the majority of full-length Gli3 ($Gli3^{FL}$) undergoes C-terminal processing to generate a repressor form ($Gli3^{Rep}$), whereas only a small fraction of full-length Gli2 ($Gli2^{FL}$) is processed ($Gli2^{Rep}$) (Pan et al., 2006; Wang et al., 2000). Gli2/Gli3 processing is induced by multi-site phosphorylation at the C-termini, first by protein kinase A (PKA) and subsequently by glycogen synthase kinase 3 (GSK3) and casein kinase 1 (CK1). Phosphorylated Gli2/Gli3 proteins are recognized and ubiquitinated by the $SCF^{\beta TrCP}$ (Skp1-Cul1-F-box protein) E3 ubiquitin ligase, and finally processed by the proteasome (Pan and Wang, 2007; Wang and Li, 2006). $Gli2^{FL}$ and $Gli3^{FL}$ shuttle between the cytoplasm and nucleus, whereas $Gli2^{Rep}$ and $Gli3^{Rep}$ reside exclusively in the nucleus. Hh signaling suppresses Gli2 and Gli3 phosphorylation and processing, thus converting $Gli2^{FL}$ and $Gli3^{FL}$ into active forms (Kim et al., 2009; Niewiadomski et al., 2014; Pan et al., 2006; Wang et al., 2000).

The primary cilium is a non-motile microtubule-based protrusion from the cell surface and is found on most vertebrate cells. Primary cilia originate in the basal body, the specialized mother centriole of the centrosome, and are elongated and maintained by intraflagellar transport (IFT), which moves proteins and vesicles into and out of the cilia (Rosenbaum and Witman, 2002). The primary cilium serves not only as a key mechanosensory organelle but also as a site for signal transduction for several signaling pathways, including the Hh pathway (Goetz and Anderson, 2010). Thus, it is not surprising that defects in cilia structure and function result in a wide spectrum of structural birth abnormalities that include eye defects, kidney cysts, craniofacial and brain malformations, heart defects, and abnormal left-right patterning diseases, which are collectively known as ciliopathies (Novarino et al., 2011). Interestingly, many of these defects are due to the disruption of Hh signaling.

In support of Hh signaling in primary cilia, Ptch1 is localized to cilia in the absence of Hh. Hh stimulation leads to the exit of Ptch1 from cilia and subsequently the accumulation of

Smo, Gli2, and Gli3 in cilia (Chen et al., 2009; Corbit et al., 2005; Haycraft et al., 2005; Rohatgi et al., 2007; Wen et al., 2010). Interestingly, Hh signaling also directs Gpr161, a ciliary localized GPCR, to be internalized from cilia. Gpr161 negatively regulates Hh signaling by increasing cAMP level, which in turn activates PKA. Consistent with this, Gli3 processing is reduced, and the Hh pathway is activated in the *Gpr161* mutant embryos (Mukhopadhyay et al., 2013). Therefore, it is generally believed that Hh signaling inhibits Gli2 and Gli3 processing and activates $Gli2^{FL}$ and $Gli3^{FL}$ proteins by suppressing their PKA phosphorylation in cilia. However, to date there is no direct evidence that this is indeed the case.

All known cilia gene mutations impair signal transduction from Smo to Gli2/Gli3. The vast majority of cilia gene mutations results in reduced Gli3 processing and thus alters $Gli3^{FL}$ and $Gli3^{Rep}$ balance, which consequently leads to polydactyly phenotype. One example is *Talpid3* (*Ta3*) mutation, which was initially identified in chicken, because the mutation results in polydactyly and central nervous system defect (Davey et al., 2006). Further studies showed that Ta3 is localized at centrioles and required for ciliogenesis (Yin et al., 2009). However, the molecular mechanisms underlying this reduced Gli3 processing in *Ta3* and any other known ciliary gene mutants are unknown. In the present study, we show that Hh signaling inhibits PKA-mediated Gli2 and Gli3 phosphorylation in cilia. The Gli2 and Gli3 phosphorylation is significantly reduced in *Ta3* mutant cells. Interestingly, Ta3 colocalizes with PKA in centrioles and interact with each other. PKA is mislocalized in some of the *Ta3* mutant cells. Therefore, our study provides evidence that Hh signaling inhibits Gli2 and Gli3 processing and activates $Gli2^{FL}$ and $Gli3^{FL}$ proteins by suppressing Gli2 and Gli3 phosphorylation in cilia. The reduced Gli2 and Gli3 processing in *Ta3* mutants is through a decrease in Gli2 and Gli3 phosphorylation, which is probably in part the result of the mislocalization of PKA in *Ta3* mutant cells.

2. Results

2.1. Hh signaling inhibits Gli2 and Gli3 phosphorylation by PKA in cilia

Gli2 and Gli3 each contain six PKA phosphorylation sites in their carboxyl (C) termini (Fig. 1A). The phosphorylation of the first four sites (P1–4) is required for Gli2 and Gli3 processing into the repressors, while phosphorylation of the fifth and sixth sites (P5–6) inhibits Gli2 and Gli3 transcriptional activity. Hh signaling inhibits Gli2 and Gli3 processing and activates $Gli2^{FL}$ and $Gli3^{FL}$ proteins by suppressing their phosphorylation (Niewiadomski et al., 2014; Pan et al., 2006, 2009; Wang et al., 2000). Although these Hh-mediated events are thought to occur in cilia, the direct evidence to support this hypothesis remains missing. To determine whether Hh signaling inhibits Gli2 and Gli3 phosphorylation in cilia, we generated an antibody (pGli) against a Gli2 peptide containing phosphorylation at the second PKA site (P2). Given that the Gli2 peptide is almost identical with Gli3 in the same region (see Materials and Methods for details), it was not surprising that this antibody weakly detected both Gli2 and Gli3 overexpressed in HEK293 cells by immunoblotting. Treatment of the cells with forskolin (Fsk), a chemical that increases cAMP levels to activate PKA, dramatically increased signals detected by the antibody, though it did not affect the levels of Gli2 and Gli3 expression shown by immunoblotting with Gli2 and Gli3 antibodies,

respectively (Fig. 1B, compare lanes 2 to 3, 7to 8). In addition, the pGli antibody failed to detect Gli2 or Gli3 mutants ($Gli2^{-P2}$ and $Gli3^{-P2}$) with a mutation at the P2 site (Fig. 1B, lanes 4–5, 9–10), indicating that Gli2 and Gli3 detected by pGli antibody in the cells without Fsk treatment are also the phosphorylated form of the proteins. Similarly, this antibody also specifically detected the phosphorylated endogenous Gli2 and Gli3 in the wild type mouse embryos, as no signal was detected in *Gli2;Gli3* double mutant embryos (Fig. 1C, compare lane 1 to lane 2). These results indicate that this antibody specifically recognizes the phosphorylated Gli2 and Gli3 at the P2 site.

Immunostaining also showed that the pGli antibody detected specific signals in cilia, as the immunofluorescence was only seen in wild type but not *Gli2;Gli3* mutant MEFs. Similarly, both Gli2 and Gli3 antibodies, which specifically recognize their C-termini (Materials and Methods), detected $Gli2^{FL}$ and $Gli3^{FL}$ proteins in cilia, respectively (Fig. 1D). Given that immunoblotting results indicate that the pGli antibody is specific only for the phosphorylated form of Gli2 and Gli3 (Fig. 1B–C), taking together, we conclude that the signals detected by the pGli antibody in cilia are the phosphorylated form of endogenous Gli2 and Gli3 at the P2 site.

Mutagenesis studies showed that all six PKA sites in the Gli2 and Gli3 C-termini are phosphorylated by PKA in the cell without noticeable preference of one to another (Pan et al., 2006; Wang et al., 2000). Hh signaling activates Gli2 and Gli3 by inducing dephosphorylation of Gli2 and Gli3 at all six PKA sites, although the extent of dephosphorylation at P5–6 is slightly more than that of P1–4 (Niewiadomski et al., 2014). Therefore, although pGli antibody recognizes Gli2 and Gli3 phosphorylated only at the P2 site, the signals detected by the antibody serve as an indicator for the extent of Gli2 and Gli3 phosphorylation at P1–6 sites by PKA.

To determine whether Hh signaling inhibits the Gli2 and Gli3 phosphorylation, the Hh-responsive C3H10T1/2 cells were incubated with or without SAG, a synthetic Smo agonist that activates the Hh pathway (Chen et al., 2002), and subjected to immunoblotting with Gli2, Gli3, and pGli antibodies. Quantification of immunoblotting results revealed that after normalized against the levels of Gli2 and Gli3, the levels of the phosphorylated Gli2 and Gli3 after SAG treatment were about 0.6 of those without treatment. Quantification of phosphorylated Gli2/Gli3 levels alone also showed a similar level of reduction in average (Fig. 2A).

To determine the dynamics of Gli2 and Gli3 phosphorylation in response to SAG, the levels of phosphorylated Gli2 and Gli3 were examined in the cells that were treated with SAG for different periods of time. A significant decrease in the levels of Gli2 and Gli3 phosphorylation, which was measured by either being normalized against Gli2 and Gli3 levels or phosphorylated Gli2/Gli3 levels alone, was seen after treatment for 6 h. Treatment for 9 and 24 h did not significantly reduce the Gli2 and Gli3 phosphorylation levels further (Fig. 2B), suggesting that the Gli2 and Gli3 dephosphorylation levels reached almost the lowest by 6 h.

We next examined the levels of phosphorylated Gli2 and Gli3 proteins in cilia in response to ShhN, an active Sonic hedgehog N-terminal fragment, or SAG stimulation by immunostaining (Fig. 2C and D). Quantification of the immunofluorescent intensity in cilia showed that after normalized against the levels of Gli2 and Gli3, the levels of the phosphorylated Gli2 and Gli3 proteins decreased about a half. When the immunofluorescent intensity of pGli staining alone was measured, the reduction of phosphorylated Gli2/Gli3 levels in cilia upon ShhN or SAG stimulation was also significant, though it was smaller (Fig. 2D, graphs). Given that Gli2 and Gli3 dephosphorylation is correlated with their activation (Niewiadomski et al., 2014), our observations support the currently prevailing hypothesis that $Gli2^{FL}$ and $Gli3^{FL}$ are activated in cilia.

2.2. Ta3 mutation results in decreased processing and phosphorylation of Gli2 and Gli3

The vast majority of ciliary gene mutations affect Gli3 processing (Goetz and Anderson, 2010), but the mechanism is unknown. To address this question, we generated a *Ta3* mutant allele in the mouse by targeted gene knockout approach (Fig. S1A–C), given that the *Ta3* mutation in chick affects ciliogenesis and Hh signaling (Davey et al., 2006). Most of *Ta3* mutant mouse embryos died around gestation day 10.5 (E10.5)($n > 30$). The development of the *Ta3* mutant embryos was often delayed (Fig. S1D). Hh signaling in *Ta3* mutants was severely impaired as demonstrated by reduced Ptch1-lacZ expression (Goodrich et al., 1997) and loss of expression of ventral neural tube markers (Foxa2, Nkx2.2, Hb9, and Isl1) (Briscoe et al., 2000) (Fig. S1E–F). As expected, no cilia formed in Ta3 mutant MEFs (Fig. S1G). These results are similar to the phenotypes of chicken and another mouse *Ta3* mutant that was previously reported (Bangs et al., 2011; Davey et al., 2006; Yin et al., 2009).

To determine whether Gli3 processing was reduced in the mouse *Ta3* mutant, protein lysates of wild type and *Ta3* mutant embryos were subjected to immunoblotting with a Gli3 N-terminal antibody, which recognizes both the $Gli3^{FL}$ and $Gli3^{Rep}$ (Wang et al., 2000). The results showed that Gli3 processing was reduced about a half in the mutant as compared to wild type (Fig. 3A).

To date, there is no evidence that Gli2 processing is also affected by ciliary gene mutations, largely because $Gli2^{Rep}$ levels are normally very low and hardly detectable (Pan et al., 2006). To overcome this obstacle, we inserted the FLAG tag in frame right after the initiation codon of Gli2 in the *Gli2* locus using targeted homologous recombination approach (Fig. 3B–C). This allele was named $Gli2^{FLAGki}$. To determine whether Gli2 processing is reduced in *Ta3* mutant embryos, the *Ta3* mutant allele was crossed into $Gli2^{FLAGki}$ mice. Immunoblotting with a FLAG antibody showed that the levels of the processed Gli2 protein, FLAG-$Gli2^{Rep}$, in *Ta3* mutant were markedly lower than those in wild type *Ta3* embryos (Fig. 3D), indicating that Gli2 processing is also impaired in *Ta3* mutant. This is the first evidence that Gli2 processing is reduced in a cilia related gene mutant.

Gli2 and Gli3 phosphorylation by PKA is essential for Gli2 and Gli3 processing (Pan et al., 2006, 2009; Wang et al., 2000). To understand the molecular basis underlying the reduced Gli2 and Gli3 processing, the levels of Gli2 and Gli3 phosphorylation were examined in the wild type and *Ta3* mutant embryos by immunoblotting. The data showed that Gli2 and Gli3

phosphorylation levels in the mutant embryos were reduced to about 0.7 of those in wild type (Fig. 4D). Thus, the reduced Gli2 and Gli3 processing is at least in part due to a decrease in Gli2 and Gli3 phosphorylation levels.

2.3. Ta3 interacts and colocalizes with PKA

To understand how *Ta3* mutation results in a decrease in Gli2 and Gli3 phosphorylation by PKA, we created NIH3T3 cells that stably expressed Ta3 tagged with FLAG and HA (FH) epitopes. Immunoaffinity purification was performed using these cells. The precipitated proteins were then subjected to mass spectrometric analysis, which showed that several tryptic peptides obtained from the precipitated proteins matched with PKA regulatory subunit type Iα, PKARIα (Fig. 4A). The interaction between Ta3 and PKARIα was confirmed by coimmunoprecipitation using Ta3 and FLAG tagged PKARIα overexpressed in HEK293 cells (Fig. 4B).

There are four PKA regulatory subunits in vertebrates, PKARIα/β and PKARIIα/β, which share a high level of sequence identity (Taylor et al., 2012). To determine whether the endogenous Ta3 interacts with one of the PKAR subunits, we chose PKARIIβ because there is a good commercial antibody available for this subunit. Ta3 antibody, but not pre-immune serum, could readily coimmunoprecipitate PKARIIβ (Fig. 4C), indicating that Ta3 also specifically interacts with PKARIIβ.

We next wanted to map the PKARIα binding region(s) in Ta3. To this end, several Ta3 mutant constructs were generated and coexpressed with FLAG-PKARIα in HEK293 cells. The protein lysates made from the cells were subjected to immunoprecipitation with either Ta3 or Myc (for Myc-tagged Ta3 mutants) antibodies, followed by immunoblotting with FLAG antibody to detect FLAG-PKARIα. The results showed that Ta3-1–470 and Ta3-1–638, the two N-terminal fragments, failed to co-precipitate FLAG-PKARIα, indicating that the N-terminal region is not sufficient to bind PKARIα. In contrast, Ta3FL (the full-length protein), Ta3-471-E-Myc (amino acid position 471 to C-terminal end), Ta3-639-E-Myc, and Ta3Δ471–638-Myc were coimmunoprecipitated with FLAG-PKARIα (Fig. 4D, two lower panels). It should be noted that less amount of FLAG-PKARIα coprecipitated with Ta3-639-E-myc is likely due to slightly lower levels of Ta3-639-E-myc expression (Fig. 4D, compare lanes 4–5 in the upper second panel). Therefore, these results indicate that the C-terminal region (639-E), but not the middle (471−638) or N-terminal regions, is required for PKARIα binding.

Given that Ta3 interacts with PKARIIβ, we next wanted to determine whether Ta3 is colocalized with PKARIIβ in the cell. Previous studies showed that both Ta3 and PKARIIβ were localized at centrioles (Kobayashi et al., 2014; Lignitto et al., 2011; Wu et al., 2014; Yin et al., 2009), but their colocalization has not been reported. Coimmunostaining wild type MEFs for Ta3 and PKARIIβ demonstrated that the two proteins indeed colocalized at centrioles. The staining for Ta3 was specific, as it was negative in *Ta3* mutant cells. The Ta3 centriolar colocalization was also observed in NIH3T3 cells (Fig. 5). Together, the data support the finding that Ta3 interacts with PKARIIβ.

2.4. Ta3 full-length protein, but not its mutants, rescues ciliogenesis in Ta3 mutant cells

To better understand the relationship between Ta3 centriolar localization and Ta3 binding to PKARIIβ, the subcellular localization of exogenous Ta3 mutant proteins and their ability to rescue ciliogenesis were examined. For this purpose, we created the same Ta3 constructs in Fig. 4E in a murine retroviral vector that contains FH epitope tags. The retroviral vector was chosen because it exhibits higher transduction efficiency and lower level of expression as compared to a CMV-promoter based plasmid. After *Ta3* mutant MEFs were separately infected with the virus carrying these constructs, the cells were co-immunostained for FH-Ta3 and its mutant proteins, Cep120 (labeling two centrioles) (Mahjoub et al., 2010), and Arl13b (a cilia marker) (Caspary et al., 2007). The results showed that only Ta3FL and Ta3-1–638, but not any other mutants, were localized at centrioles (Fig. 6A–G). The lack of centriolar localization of these mutants was not the results of the failed protein expression, since immunoblotting analysis showed that they were expressed (Fig. 6I). Interestingly, 60% of the cells in which FH-Ta3 localized at centrioles formed cilia, whereas none of the cells in which FH-Ta3-1–638 localized to centrioles generated any cilia (Fig. 6H). Therefore, the Ta3 full-length protein is required for the rescue of ciliogenesis, and Ta3-1–638 is responsible for Ta3 centriolar localization.

2.5. PKARIIβ is not localized at centrosome in some of Ta3 mutant cells

PKARIIβ is normally concentrated at Golgi-centrosome and perinuclear region (Lignitto et al., 2011). So is the A-kinase anchoring protein AKAP9 (Larocca et al., 2004; Schmidt et al., 1999). To understand the molecular and cellular mechanisms by which Gli2 and Gli3 phosphorylation is reduced in *Ta3* mutant cells, PKARIIβ subcellular localization in both wild type and *Ta3* mutant cells were investigated. As expected, PKARIIβ was colocalized with AKAP9 to centrosome-Golgi in all the wild type cells examined (Fig. 7As). However, PKARIIβ was not colocalized with AKAP9 in about a quarter of *Ta3* mutant cells (Fig. 7Bs and D, no colocalization, left inset; colocalization, right inset). The absence of PKARIIβ at centrosome was not because of the difference in the protein levels between wild type and *Ta3* mutant cells, as shown by immunoblot (Fig. 7E). This was also specific for *Ta3* mutant cells, as PKARIIβ was normally localized at centrosome and Golgi in *Dzip1* (a ciliary gene encoding a centrosomal protein) mutant cells that also lack cilia (Wang et al., 2013). Thus, *Ta3* mutation disrupts PKARIIβ localization to centrosome-Golgi at least in some cells.

3. Discussion

In the present study, we show that Hh signaling inhibits Gli2 and Gli3 phosphorylation by PKA in cilia. *Ta3* mutation also results in decrease in the processing and phosphorylation of both Gli2 and Gli3. It should be noted that this is the first time to show that Gli2 processing is impaired in a ciliary gene mutant. Ta3 interacts and colocalizes with PKA regulatory subunits at the centrosome. Interestingly, PKARIIβ is not localized at the centrosome in some of the *Ta3* mutant MEFs. Our findings provide the direct evidence that Hh-dependent Gli2 and Gli3 dephosphorylation occurs in cilia and support the hypothesis that the reduced Gli2 and Gli3 processing in *Ta3* mutant is due to a decrease in Gli2 and Gli3 phosphorylation probably partially resulted from PKARIIβ mislocalization.

It is generally believed that Hh signaling occurs in cilia. In the absence of Hh signaling, both Ptch1, the Hh receptor that inhibits Smo activity, and Gpr161, a GPCR that antagonizes Hh signaling by activating PKA, are localized to cilia. Hh signaling results in the removal of Ptch1 and Gpr161 from cilia (Mukhopadhyay et al., 2013; Rohatgi et al., 2007) and concomitantly the accumulation of Smo, Gli2, and Gli3 in cilia (Chen et al., 2009; Corbit et al., 2005; Haycraft et al., 2005; Wen et al., 2010). Hh signaling ultimately inhibits Gli2 and Gli3 processing that generates repressors and converts $Gli2^{FL}$ and $Gli3^{FL}$ into activators. Given that Gli2 and Gli3 processing is dependent on the phosphorylation by PKA at P1–4 sites (Pan et al., 2006; Wang et al., 2000), whereas their activation is associated with dephosphorylation of all six PKA sites P1–6 or PKA gene mutations (Niewiadomski et al., 2014; Tuson et al., 2011), understanding where and how Gli2 and Gli3 are phosphorylated and dephosphorylated is greatly important. Here we show that Hh signaling inhibits Gli2 and Gli3 phosphorylation in cilia (Fig. 2C–D) and provide the first direct evidence that Gli2 and Gli3 are activated in cilia.

Most of the *Ta3* mutant phenotypes, including polydactyly and the lack of the specification of ventral neural cell types in the neural tube, are the result of the failed activation and reduced processing of $Gli2^{FL}$ and $Gli3^{FL}$ proteins (Fig. S1E and F, 3A and D)(Bangs et al., 2011; Davey et al., 2006). It is not known how Gli2 and Gli3 processing is impaired and why $Gli2^{FL}$ and $Gli3^{FL}$ are inactive in *Ta3* and, in fact, any other known ciliary gene mutants. We demonstrate here that Gli2 and Gli3 phosphorylation is reduced in *Ta3* mutant (Fig. 3E). This explains why Gli2 and Gli3 processing is impaired in the mutant. However, this does not explain why $Gli2^{FL}$ and $Gli3^{FL}$ are inactive, since the decrease in phosphorylation has been shown to be associated with $Gli2^{FL}$ and $Gli3^{FL}$ activation and thus is expected to increase $Gli2^{FL}$ and $Gli3^{FL}$ activity (Niewiadomski et al., 2014). Therefore, $Gli2^{FL}$ and $Gli3^{FL}$ activation needs more than just dephosphorylation. For example, desumoylation and acetylation of Gli2 and Gli3 are likely required, as they have been shown to increase Gli2 and Gli3 activity (Han et al., 2012). In addition, the translocation of $Gli2^{FL}$ and $Gli3^{FL}$ into the nucleus is another mechanism essential for Gli2 and Gli3 activation by Hh signaling (Kim et al., 2009; Niewiadomski et al., 2014), which could be altered in Ta3 mutant cells.

The C-terminally truncated Ta3-1-638 is localized to centrioles, but fails to restore ciliogenesis. Ta3-471-E neither localizes at centrioles nor rescues ciliogenesis. Not only can Ta3FL rescue ciliogenesis but also localizes at centrioles (Fig. 6As, Cs, and Ds). These results indicate that the N-terminal region determines Ta3 centriolar localization, while the C-terminal region is required for ciliogenesis. The Ta3 centriolar localization is dependent on the C-terminal region (471-638aa) of the N-terminal fragment, as both Ta3Δ471–636 and Ta3-1-470 fail to localize at centrioles. However, Ta3-471-638 is not sufficient to direct Ta3 to the centrioles in MEFs (Fig. 6Ds, Fs, and Gs). The observation that Ta3-471-E fails to rescue ciliogenesis is inconsistent with a previous study showing that a similar Ta3 mutant was able to rescue ciliogenesis in chick embryos (Yin et al., 2009). The discrepancy between the two studies may be due to the experimental systems used—MEFs versus chick embryos, or the sequence difference in the mouse and chick Ta3 proteins. Additional studies are needed to distinguish between the two possibilities.

Ta3 is the first known ciliary protein that is shown to bind PKA. The PKA binding region is mapped to the Ta3 C-terminal region (Fig. 4D and E). In support of the interaction between Ta3 and PKA, the Ta3 and PKARIIβ colocalize at centrioles (Fig. 5). Thus, Ta3 serves as an AKAP to coordinate PKA-dependent Gli2 and Gli3 phosphorylation. Loss of *Ta3* results in decrease in the Gli2 and Gli3 phosphorylation (Fig. 3E). The observation that PKARIIβ is absent at centrosome and Golgi in some of *Ta3* mutant MEFs suggests that PKARIIβ mislocalization at least partially accounts for the reduced Gli2 and Gli3 phosphorylation in *Ta3* mutant cells. This is specific for *Ta3* mutant, since PKARIIβ centriolar localization is normal in *Dzip1* and other ciliary gene mutant cells examined (Fig. 7, data not shown). We currently do not know why PKARIIβ mislocalization is found only in some of the *Ta3* mutant cells. One possibility is that given that *Ta3* mutant MEFs are heterogeneous, *Ta3* mutation may affect PKARIIβ localization to different extent depending on cell types. It is possible that PKARIIβ localization has also been altered in the *Ta3* mutant cells that seem to have normal PKARIIβ localization. Such alteration is just too subtle to be clearly detected by immunostaining. Further studies are necessary to determine why PKARIIβ fails to localize at centrioles in only some of *Ta3* mutant cells.

4. Materials and methods

4.1. Mouse strains and the generation of a Ta3 mutant and Gli2-FLAGki alleles

BAC clones containing mouse *Ta3* or *Gli2* genomic DNA sequences were purchased from the BACPAC Resources Center (Oakland, CA, USA) and used to create *Ta3* or $Gli2^{FLAGki}$ targeting constructs. The *Ta*3 construct was engineered by replacing the first three exons of the *Ta3* gene with the pGKneo cassette flanked by loxP sites (Soriano, 1997) (Fig. S1A). The $Gli2^{FLAGki}$ construct was generated by inserting 3×FLAG and pGKneo cassette into the first ATG and first *Avr*II restriction site right after the first exon of the *Gli2* locus, respectively (Fig. 3B). The linearized constructs were electroporated into W4 ES cells (Taconic Biosciences). The targeted *Ta3* mutant ES cell clones were identified by digestion of ES cell genomic DNA with *Eco*RV (5′ homologous arm) or *Bgl*II (3′ homologous arm), followed by a Southern blot analysis using two probes as indicated (Fig. S1B). The targeted $Gli2^{FLAGki}$ mutant ES cell clones were determined by digestion of genomic DNA with *Bam*HI, followed by a Southern blot analysis with two different probes, one for 5′- and the other for 3′-homologous recombination (Fig. 3B and C). Two for each of *Ta3* and $Gli2^{FLAGki}$ targeted ES cell clones were injected into C57BL/6 blastocysts to generate chimeric founders, which were then bred with C57BL/6 to establish F1 heterozygotes. The *Ta3* mutant heterozygotes and $Gli2^{FLAGki}$ homozygotes were maintained in 129/SVE, C57BL/6, and SW mix background. PCR (polymerization chain reaction) analysis was used for routine genotyping *Ta3* with the following primers: forward primer BW725F, 5′-GTGATTATCTGTTCGTCAGTGC-3′ and reverse prime BW725R, 5′-CGCCTTTATGTTTGGACACAGT −3′ for the wild type (wt) *Ta3* allele, which produced a 220 bp fragment; and forward primer BW725F and reverse primer BW128, 5′-TGCTAAAGCGCATGCTCCAG-3′ on pGKneo for the targeted *Ta3* allele, which produced a 260 bp fragment. The primers used to genotyping $Gli2^{FLAGki}$ are BW573F, 5′-TGTCTGTGTCCTTTCCTCCAG-3′, and BW709R, 5′-GCAGAGGCACTGCCCTCCATA-3′, to produce a 300 bp fragment for wt and a 370 bp

fragment for *Gli2*^{FLAGki}. The animal work was approved by Institutional Animal Care and Use Committee at Weill Medical College.

4.2. Cell lines and cell culture

Wild type (wt), *Ta3*, and *Gli2;Gli3* mutant primary mouse embryonic fibroblasts (pMEFs) were prepared from E11.5 or E12.5 mouse embryos. The pMEFs were cultured in DMEM supplemented with 10% FBS (fetal bovine serum)(Atlanta Biologicals), penicillin, and streptomycin (Corning). The immortalized wt and *Ta3* mutant MEFs were generated by incubating the pMEFs in the same growth medium at the higher density for many passages until the cells passed crises and gained normal growth rate. HEK293 and C3H10T1/2 cells were originally obtained from ATCC and incubated in the same growth medium. NIH3T3 obtained from Xin-Yun Huang lab at Weill Medical College and its related cells were grown in DMEM supplemented with 10% calf serum (CS), penicillin, and streptomycin. Mycoplasma test was completed when the cells lines were received and was negative. To make ShhN conditioned medium, a pRK-ShhN expression construct was transfected into HEK293cells by calcium phosphate precipitation method (Wang et al., 2000). Two days post-transfection, the medium was collected. ShhN conditioned medium (1:10 dilution) and SAG (300 nM) (Cayman Chemical) were used to stimulate C3H10T1/2 for overnight or times as indicated. To induce Gli2 and Gli3 phosphorylation by PKA, the transfected HEK293cells were incubated with either vehicle (DMSO control) or Forskolin (Fsk, 40 μM) (Calbiochem) for 1.5 h before the cells were lysed.

4.3. cDNA constructs, cloning, and transfection

The mouse *Ta3* full-length cDNA was created by combining three cDNA fragments that were amplified from a cDNA library by PCR. Murine retroviral pLNCX-FH-Ta3 or its mutant cDNA constructs (numbers are amino acid positions) were created by inserting the cDNA fragments into pLNCX-FH retroviral vector by PCR and general cloning techniques. pLNCX-FH was engineered by inserting FH, FLAG and HA double tags, into pLNCX (Clontech). pRK-Ta3 and its mutant cDNA constructs were generated by inserting the cDNA fragments into a CMV based pRK or pRK-myc vector using PCR and general molecular cloning techniques. PKARIα cDNA was amplified from a mouse cDNA library by PCR and inserted into the pCMV-FLAG (Sigma) vector to create pCMV-FLAG-PKARIα. The constructs were verified by DNA sequencing. Virus carrying FH-Ta3 or its mutant constructs was generated by cotransfecting Phoenix-Eco cells (ATCC) with each of the viral constructs and pEco packaging construct using the calcium phosphate precipitation method (Wang et al., 2013). pRK-Gli2, pRK-Gli3, pRK-Gli2-P2, pRK-Gli3-P2 were described previously (Pan et al., 2006; Wang et al., 2000).

4.4. Embryo section immunofluorescence and whole mount lacZ staining

For immunofluorescence of neural tube sections, mouse embryos at 10.5 days post coitus (E10.5) were dissected, fixed in 4% paraformaldehyde (PFA)/PBS for 1 h at 4 °C, equilibrated in 30% sucrose/PBS overnight at 4 °C, and embedded in OCT. The frozen embryos were transversely cryosectioned at the forelimb areas (10 μm/section). Tissue sections were immunostained with antibodies against Foxa2 (concentrated), Nks2.2, Hb9, Isl1, Pax6 (Developmental Study Hybridoma Bank (DSHB), Iowa) as described (Pan et al.,

2009). Whole mount lacZ staining of mouse embryos was performed as described (Hogan et al., 1994).

4.5. Immunofluorescence and Microscopy

For cell ciliation studies, cells were plated on coverslips coated with 0.1% gelatin for at least overnight and serum starved with 0.1% FBS for 24 h to arrest the cells. For centrosome staining, cells were fixed in −20 °C cold methanol for 5 mins. For the cytoplasmic and cilia staining, cells were fixed in 4% PFA/PBS for 15 mins. After washed with PBS, the cells were incubated with blocking solution (PBS/0.2% Triton X-100/4% heat inactivated calf serum) for 20 mins. The cells were then incubated with primary antibodies in blocking solution for 1 h at room temperature. The cells were washed with PBS, incubated with secondary antibodies in blocking solution for 1 h at room temperature. After wash three times with PBS, the coverslips were mounted to glass slides with Vectashield mounting fluid with DAPI (Vector Labs). The staining was visualized using a Zeiss Axiovert fluorescent microscope. The fluorescence intensity in cilia was quantified using NIH imageJ. Two-tailed Student *t*-test was used to calculate p-values.

4.6. Antibodies

Arl13b, AKAP9, Gli2, Gli3, and pGli antibodies were generated by Covance or Biosynthesis. Rabbits were immunized with purified bacterially expressed His-tagged mouse Arl13b, His-tagged mouse AKAP9 fragment (2768–3116 aa), His-tagged mouse Gli2C-terminal fragment (605–1460 aa), GST-tagged Gli3 C-terminal fragment (1051–1179 aa), or the synthetic Gli2P2 phospho-peptide (NH_2-CAYTVSRRS-(pS)-GISP-OH), in which residue C is not from Gli2 and was used for conjugation of the peptide to Keyhole Limpet Hemocyanin (KLH). It is worth noting that the sequence for Gli3 in the same region is AYLSSRRSSGISP with only the 3rd and 4th residues different from the Gli2. The phosphorylation site is conserved between Gli2 and Gli3. The antibodies were used in a 1:1000 dilution. Other antibodies include: Gli2 N-terminal, Gli3 N-terminal, Ta3, Cep120 (all 1:1000) (Pan et al., 2006; Wang et al., 2000; Wu et al., 2014), acetylated tubulin (1:4000), FLAG (T6793, F1804, Sigma), PKARIIβ (610625, BD Biosciences), and Myc (sc-788, Santa Cruz Biotechnology). Secondary antibodies Alexa Fluor 488-conjugated goat anti-rabbit IgG (111−545-144) and Cy3-conjugated goat anti-mouse IgG (115−165-146) were purchased from Jackson Immunoresearch, Inc.

4.7. Immunoblotting, coimmunoprecipitation, immunoaffinity purification, and mass spectrometry analysis

E10.5 mouse embryos used to detect FLAG-Gli2 or Gli3 were lysed in RIPA buffer (50 mM Tris-HCl [pH 7.4], 150 mM NaCl, 1 mM EDTA, 1%Triton X-100, 1% sodium deoxycholate, 0.1% SDS, protease inhibitors). Cultured cells used to detect Ta3, PKARIα, PKARIIβ were lysed in lysis buffer (50 mM HEPES (pH7.4), 150 mM NaCl, 10% glycerol, 1% NP40, protease inhibitors). Immunoblotting and coimmunoprecipitation were performed as described (Wang et al., 2000). The intensity of immunoblot bands was quantified using NIH imageJ. Two-tailed Student *t*-test was used to determine p-values.

For immunoaffinity purification, twenty 15 cm plates of NIH3T3 cells stably transduced with pLNCX-FH-Ta3 virus or NIH3T3control cells were lysed by Dounce homogenization in lysis buffer (50 mM HEPES (pH7.4), 150 mM NaCl, 10% glycerol, 0.5% NP40, freshly add DTT (1 mM), protease inhibitor cocktail). After cleared by centrifugation, the protein lysates were incubated with 200 μl FLAG antibody conjugated with Sepharose beads (A2220, Sigma) by rotation for 2 h at 4 °C. The beads were washed with the lysis buffer for at least 4 times. The immunoprecipitated proteins were denatured with SDS loading buffer and resolved by SDS-PAGE. The gel lanes were sliced into 8 pieces, which were subjected to digestion with trypsin. The resulting peptides were eluted and subjected to mass spectrometric analysis as described (Xu et al., 2010).

Supplementary Material

Refer to Web version on PubMed Central for supplementary material.

Acknowledgments

We thank Yong Pan for helping characterize the pGli antibody. Monoclonal antibodies, Foxa2, Isl1, Hb9, and Pax6 were purchased from the Developmental Studies Hybridoma Bank maintained by the University of Iowa, Department of Biological Sciences, Iowa City, Iowa 52242, under contract NO1-HD-7–3263 from the NICHD. This study was supported by National Institutes of Health (USA) (R01GM114429) to B.W., National Natural Science Foundation of China (31570721), Chinese Ministry for Foreign Experts (GDW20143100069), and Science and Technology Commission of Shanghai Municipality (14521100700 and 14520720200) to Q.M., National Natural Science Foundation of China (31470772) and Jiangsu Key Laboratory of Translational Research and Therapy for Neuro-Psycho-Diseases (BM2013003) to G.X. J.L. is a recipient of Scholarship from Chinese Scholarship Council.

References

Bai CB, Stephen D, Joyner AL. All mouse ventral spinal cord patterning by hedgehog is Gli dependent and involves an activator function of Gli3. Dev. Cell. 2004; 6:103–115. [PubMed: 14723851]

Bangs F, Antonio N, Thongnuek P, Welten M, Davey MG, Briscoe J, Tickle C. Generation of mice with functional inactivation of talpid3, a gene first identified in chicken. Development. 2011; 138:3261–3272. [PubMed: 21750036]

Briscoe J, Pierani A, Jessell TM, Ericson J. A homeodomain protein code specifies progenitor cell identity and neuronal fate in the ventral neural tube. Cell. 2000; 101:435–445. [PubMed: 10830170]

Caspary T, Larkins CE, Anderson KV. The graded response to Sonic Hedgehog depends on cilia architecture. Dev. Cell. 2007; 12:767–778. [PubMed: 17488627]

Chen JK, Taipale J, Young KE, Maiti T, Beachy PA. Small molecule modulation of Smoothened activity. Proc. Natl. Acad. Sci. Usa. 2002; 99:14071–14076. [PubMed: 12391318]

Chen MH, Wilson CW, Li YJ, Law KK, Lu CS, Gacayan R, Zhang X, Hui CC, Chuang PT. Cilium-independent regulation of Gli protein function by Sufu in Hedgehog signaling is evolutionarily conserved. Genes Dev. 2009; 23:1910–1928. [PubMed: 19684112]

Corbit KC, Aanstad P, Singla V, Norman AR, Stainier DY, Reiter JF. Vertebrate smoothened functions at the primary cilium. Nature. 2005; 437:1018–1021. [PubMed: 16136078]

Davey MG, Paton IR, Yin Y, Schmidt M, Bangs FK, Morrice DR, Smith TG, Buxton P, Stamataki D, Tanaka M, Munsterberg AE, Briscoe J, Tickle C, Burt DW. The chicken talpid3 gene encodes a novel protein essential for Hedgehog signaling. Genes Dev. 2006; 20:1365–1377. [PubMed: 16702409]

Fuse N, Maiti T, Wang B, Porter JA, Hall TM, Leahy DJ, Beachy PA. Sonic hedgehog protein signals not as a hydrolytic enzyme but as an apparent ligand for patched. Proc. Natl. Acad. Sci. USA. 1999; 96:10992–10999. [PubMed: 10500113]

Goetz SC, Anderson KV. The primary cilium: a signalling centre during vertebrate development. Nat. Rev. 2010; 11:331–344.

Goodrich LV, Johnson RL, Milenkovic L, McMahon JA, Scott MP. Conservation of the hedgehog/patched signaling pathway from flies to mice: induction of a mouse patched gene by Hedgehog. Genes Dev. 1996; 10:301–312. [PubMed: 8595881]

Goodrich LV, Milenkovic L, Higgins KM, Scott MP. Altered neural cell fates and medulloblastoma in mouse patched mutants. Science. 1997; 277:1109–1113. [PubMed: 9262482]

Han L, Pan Y, Wang B. Small ubiquitin-like Modifier (SUMO) modification inhibits GLI2 protein transcriptional activity in vitro and in vivo. J. Biol. Chem. 2012; 287:20483–20489. [PubMed: 22549777]

Haycraft CJ, Banizs B, Aydin-Son Y, Zhang Q, Michaud EJ, Yoder BK. Gli2 and Gli3 localize to cilia and require the intraflagellar transport protein polaris for processing and function. PLoS Genet. 2005; 1:e53. [PubMed: 16254602]

Hogan, B., Beddington, R., Costantini, F., Lacy, E. Manipulating the Mouse Embryos—A Laboratory Manual Second edition. Cold Spring Harbor Laboratory Press, USA; 1994.

Jiang J, Hui CC. Hedgehog signaling in development and cancer. Dev. Cell. 2008; 15:801–812. [PubMed: 19081070]

Kim J, Kato M, Beachy PA. Gli2 trafficking links Hedgehog-dependent activation of Smoothened in the primary cilium to transcriptional activation in the nucleus. Proc. Natl. Acad. Sci. USA. 2009; 106:21666–21671. [PubMed: 19996169]

Kobayashi T, Kim S, Lin YC, Inoue T, Dynlacht BD. The CP110-interacting proteins Talpid3 and Cep290 play overlapping and distinct roles in cilia assembly. J. Cell Biol. 2014; 204:215–229. [PubMed: 24421332]

Larocca MC, Shanks RA, Tian L, Nelson DL, Stewart DM, Goldenring JR. AKAP350 interaction with cdc42 interacting protein 4 at the Golgi apparatus. Mol. Biol. Cell. 2004; 15:2771–2781. [PubMed: 15047863]

Lignitto L, Carlucci A, Sepe M, Stefan E, Cuomo O, Nistico R, Scorziello A, Savoia C, Garbi C, Annunziato L, Feliciello A. Control of PKA stability and signalling by the RING ligase praja2. Nat. Cell Biol. 2011; 13:412–422. [PubMed: 21423175]

Mahjoub MR, Xie Z, Stearns T. Cep120 is asymmetrically localized to the daughter centriole and is essential for centriole assembly. J. Cell Biol. 2010; 191:331–346. [PubMed: 20956381]

Marigo V, Johnson RL, Vortkamp A, Tabin CJ. Sonic hedgehog differentially regulates expression of GLI and GLI3 during limb development. Dev. Biol. 1996; 180:273–283. [PubMed: 8948590]

Mukhopadhyay S, Wen X, Ratti N, Loktev A, Rangell L, Scales SJ, Jackson PK. The ciliary G-protein-coupled receptor Gpr161 negatively regulates the Sonic hedgehog pathway via cAMP signaling. Cell. 2013; 152:210–223. [PubMed: 23332756]

Niewiadomski P, Kong JH, Ahrends R, Ma Y, Humke EW, Khan S, Teruel MN, Novitch BG, Rohatgi R. Gli protein activity is controlled by multisite phosphorylation in vertebrate Hedgehog signaling. Cell Rep. 2014; 6:168–181. [PubMed: 24373970]

Novarino G, Akizu N, Gleeson JG. Modeling human disease in humans: the ciliopathies. Cell. 2011; 147:70–79. [PubMed: 21962508]

Pan Y, Bai CB, Joyner AL, Wang B. Sonic hedgehog signaling regulates Gli2 transcriptional activity by suppressing its processing and degradation. Mol. Cell. Biol. 2006; 26:3365–3377. [PubMed: 16611981]

Pan Y, Wang B. A novel protein-processing domain in Gli2 and Gli3 differentially blocks complete protein degradation by the proteasome. J. Biol. Chem. 2007; 282:10846–10852. [PubMed: 17283082]

Pan Y, Wang C, Wang B. Phosphorylation of Gli2 by protein kinase A is required for Gli2 processing and degradation and the Sonic Hedgehog-regulated mouse development. Dev. Biol. 2009; 326:177–189. [PubMed: 19056373]

Riobo NA, Saucy B, Dilizio C, Manning DR. Activation of heterotrimeric G proteins by Smoothened. Proc. Natl. Acad. Sci. USA. 2006; 103:12607–12612. [PubMed: 16885213]

Rohatgi R, Milenkovic L, Scott MP. Patched1 regulates hedgehog signaling at the primary cilium. Science. 2007; 317:372–376. [PubMed: 17641202]

Rosenbaum JL, Witman GB. Intraflagellar transport. Nat. Rev. Mol. Cell Biol. 2002; 3:813–825. [PubMed: 12415299]

Schmidt PH, Dransfield DT, Claudio JO, Hawley RG, Trotter KW, Milgram SL, Goldenring JR. AKAP350, a multiply spliced protein kinase A-anchoring protein associated with centrosomes. J. Biol. Chem. 1999; 274:3055–3066. [PubMed: 9915845]

Soriano P. The PDGF alpha receptor is required for neural crest cell development and for normal patterning of the somites. Development. 1997; 124:2691–2700. [PubMed: 9226440]

Stone DM, Hynes M, Armanini M, Swanson TA, Gu Q, Johnson RL, Scott MP, Pennica D, Goddard A, Phillips H, Noll M, Hooper JE, de Sauvage F, Rosenthal A. The tumour-suppressor gene patched encodes a candidate receptor for Sonic hedgehog. Nature. 1996; 384:129–134. [PubMed: 8906787]

Taylor SS, Ilouz R, Zhang P, Kornev AP. Assembly of allosteric macromolecular switches: lessons from PKA. Nat. Rev. Mol. Cell Biol. 2012; 13:646–658. [PubMed: 22992589]

Tuson M, He M, Anderson KV. Protein kinase A acts at the basal body of the primary cilium to prevent Gli2 activation and ventralization of the mouse neural tube. Development. 2011; 138:4921–4930. [PubMed: 22007132]

Wang B, Fallon JF, Beachy PA. Hedgehog-regulated processing of Gli3 produces an anterior/posterior repressor gradient in the developing vertebrate limb. Cell. 2000; 100:423–434. [PubMed: 10693759]

Wang B, Li Y. Evidence for the direct involvement of {beta}TrCP in Gli3 protein processing. Proc. Natl. Acad. Sci. USA. 2006; 103:33–38. [PubMed: 16371461]

Wang C, Low WC, Liu A, Wang B. Centrosomal protein DZIP1 regulates Hedgehog signaling by promoting cytoplasmic retention of transcription factor GLI3 and affecting ciliogenesis. J. Biol. Chem. 2013; 288:29518–29529. [PubMed: 23955340]

Wen X, Lai CK, Evangelista M, Hongo JA, de Sauvage FJ, Scales SJ. Kinetics of hedgehog-dependent full-length Gli3 accumulation in primary cilia and subsequent degradation. Mol. Cell. Biol. 2010; 30:1910–1922. [PubMed: 20154143]

Wu C, Yang M, Li J, Wang C, Cao T, Tao K, Wang B. Talpid3-binding centrosomal protein Cep120 is required for centriole duplication and proliferation of cerebellar granule neuron progenitors. PloS One. 2014; 9:e107943. [PubMed: 25251415]

Xu G, Paige JS, Jaffrey SR. Global analysis of lysine ubiquitination by ubiquitin remnant immunoaffinity profiling. Nat. Biotechnol. 2010; 28:868–873. [PubMed: 20639865]

Yin Y, Bangs F, Paton IR, Prescott A, James J, Davey MG, Whitley P, Genikhovich G, Technau U, Burt DW, Tickle C. The Talpid3 gene (KIAA0586) encodes a centrosomal protein that is essential for primary cilia formation. Development. 2009; 136:655–664. [PubMed: 19144723]

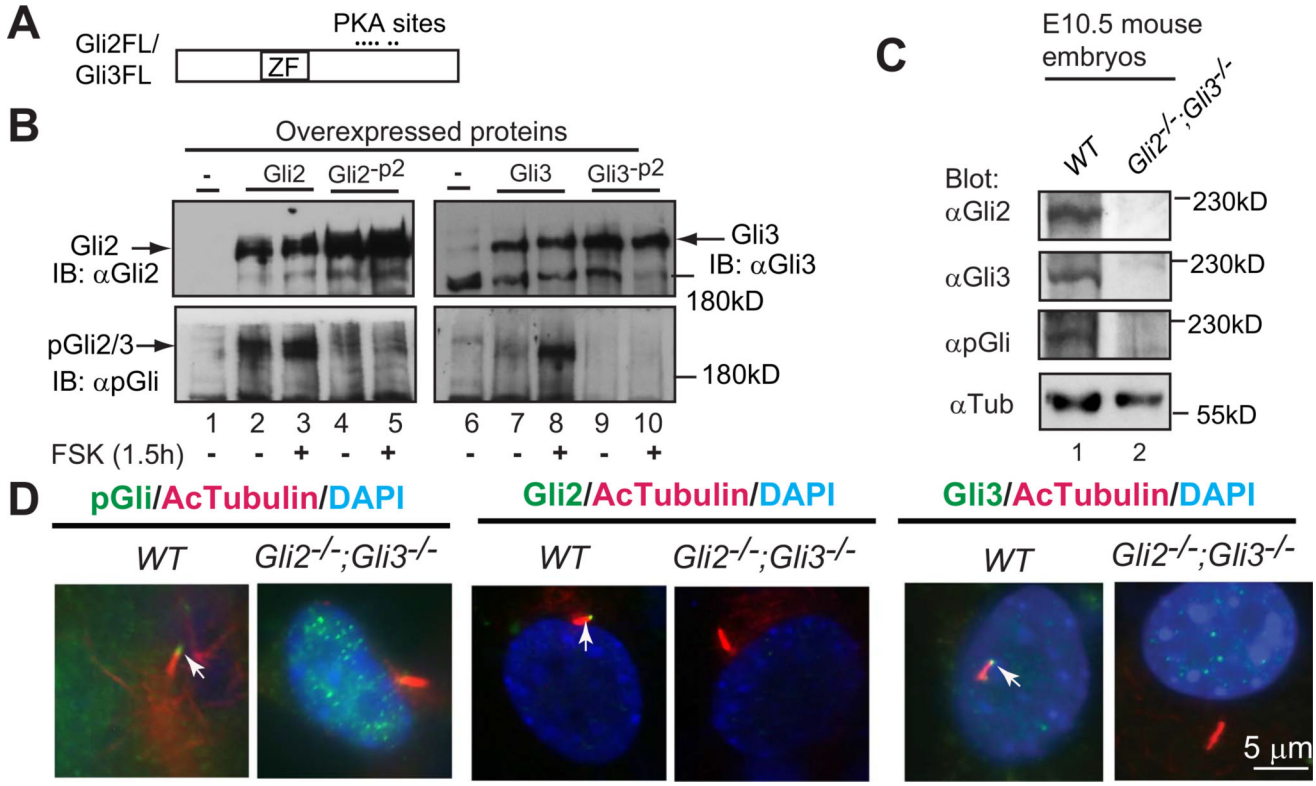

Fig. 1.

A phosphopeptide antibody (pGli) specifically recognizes the phosphorylated Gli2 and Gli3 proteins at the second PKA site. (**A**) A diagram showing Gli2 and Gli3 proteins with the zinc-finger domain (ZF) and six PKA sites. (**B**) Immunoblots of overexpressed Gli2, Gli3, and their mutants at the second PKA site (Gli2-P2, Gli3-P2) with Gli2, Gli3, or pGli antibodies. Forskolin (FSK) induces Gli2/Gli3 phosphorylation. (**C**) Immunoblots of endogenous Gli2, Gli3, and phosphorylated Gli2/Gli3 using protein lysates prepared from wild type (WT) and *Gli2;Gli3* double mutant (control) mouse embryos. (**D**) Gli2, Gli3, and PKA-phosphorylated Gli2 and Gli3 localize to primary cilia. Immunostaining of WT and *Gli2;Gli3* double mutant MEFs for the indicated proteins. Note that pGli, Gli2, and Gli3 antibodies are specific, as no signals were detected in the protein lysates and cilia of the mutant cells. AcTubulin, acetylated tubulin, a cilia marker; DAPI, staining for nuclei. These experiments were performed at least two times.

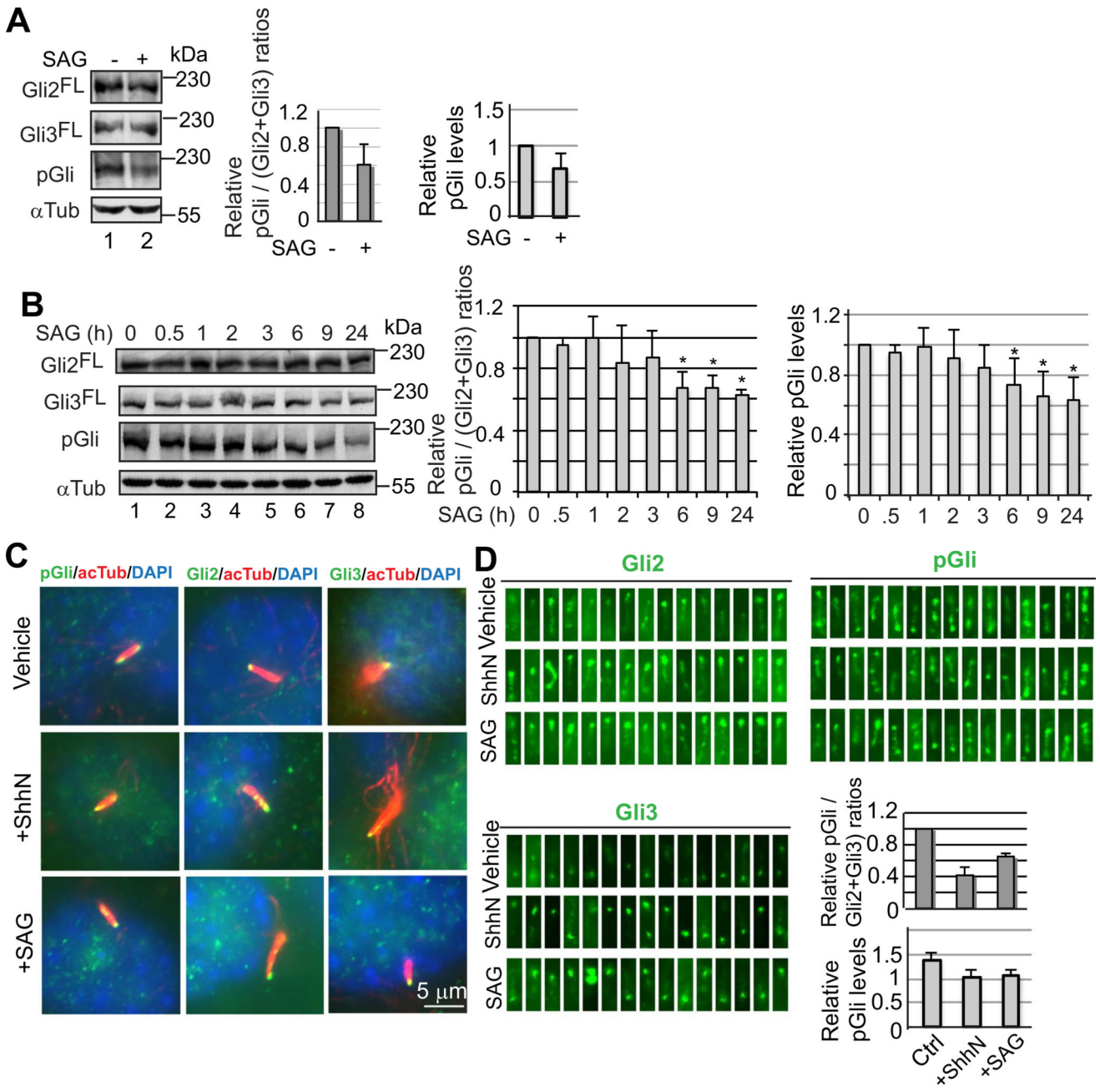

Fig. 2.

Hedgehog signaling inhibits PKA-mediated Gli2 and Gli3 phosphorylation in cilia. (**A**) Immunoblots showing the levels of $Gli2^{FL}$, $Gli3^{FL}$, and phosphorylated Gli2 and Gli3 (pGli) in C3H10T1/2 cells. Graphs show the relative pGli levels either with or without being normalized to those of Gli2FL and Gli3FL. Two-tailed Student *t*-test p-value = 0.034 < 0.5. (**B**) Immunoblots showing the time course of the levels of $Gli2^{FL}$, $Gli3^{FL}$, and pGli in response to SAG. Graphs to the right show the relative pGli/(Gli2+Gli3) or pGli values. P-values ≤ 0.0067 for bar graphs marked with *. (**C**) Representative images showing Gli2, Gli3, and pGli staining in cilia before and after treatment with ShhN or SAG. (**D**) Fifteen randomly chosen cilia that show positive staining for Gli2, Gli3, and pGli. The graphs show

the arbitrary intensity of pGli staining per cilia by either with (upper graph) or without (lower graph) being normalized against $Gli2^{FL}$ and $Gli3^{FL}$ levels. Two-tailed Student *t*-test p-value ≤ 0.00057 (upper graph) or 0.036 (lower graph), respectively.

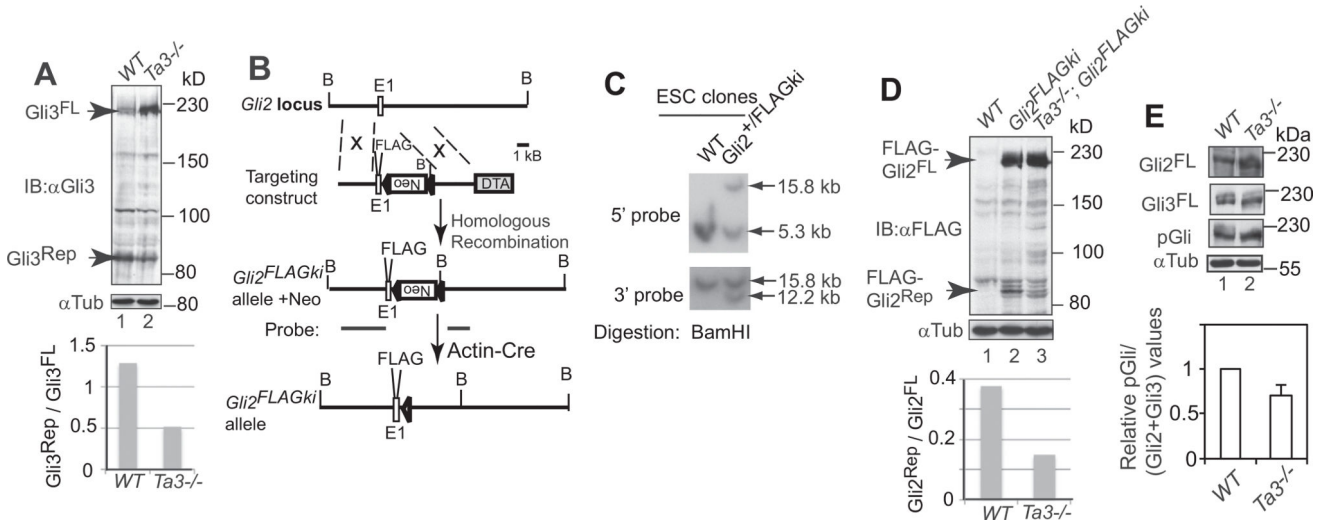

Fig. 3.

The processing and PKA-mediated phosphorylation of Gli2 and Gli3 were diminished in *Ta3* mutant cells. (**A, D, E**) Immunoblots for Gli3, FLAG-Gli2, Gli2, and pGli in wt and *Ta3* mutant embryos. Tubulin immunoblots are loading controls. Graphs show the ratios of $Gli3^{Rep}$ to $Gli3^{FL}$ and FLAG-$Gli2^{Rep}$ to FLAG-$Gli2^{FL}$ and relative pGli to (Gli2+ Gli3) values. Two-tailed Student *t*-test p-value = 0.0136 for **E**. from three independent experiments. (**B**) The gene targeting strategy to create $Gli2^{FLAGki}$ allele. E1, exon 1; FLAG, 3×FLAG tag; Neo, pGkneo cassette in a reverse orientation; triangle, loxP site; DTA, diphtheria toxin A; B, *Bam*HI site. (**C**) Southern blot showing wt and a representative $Gli2^{FLAGki}$ ES cell clone with probes shown in B.

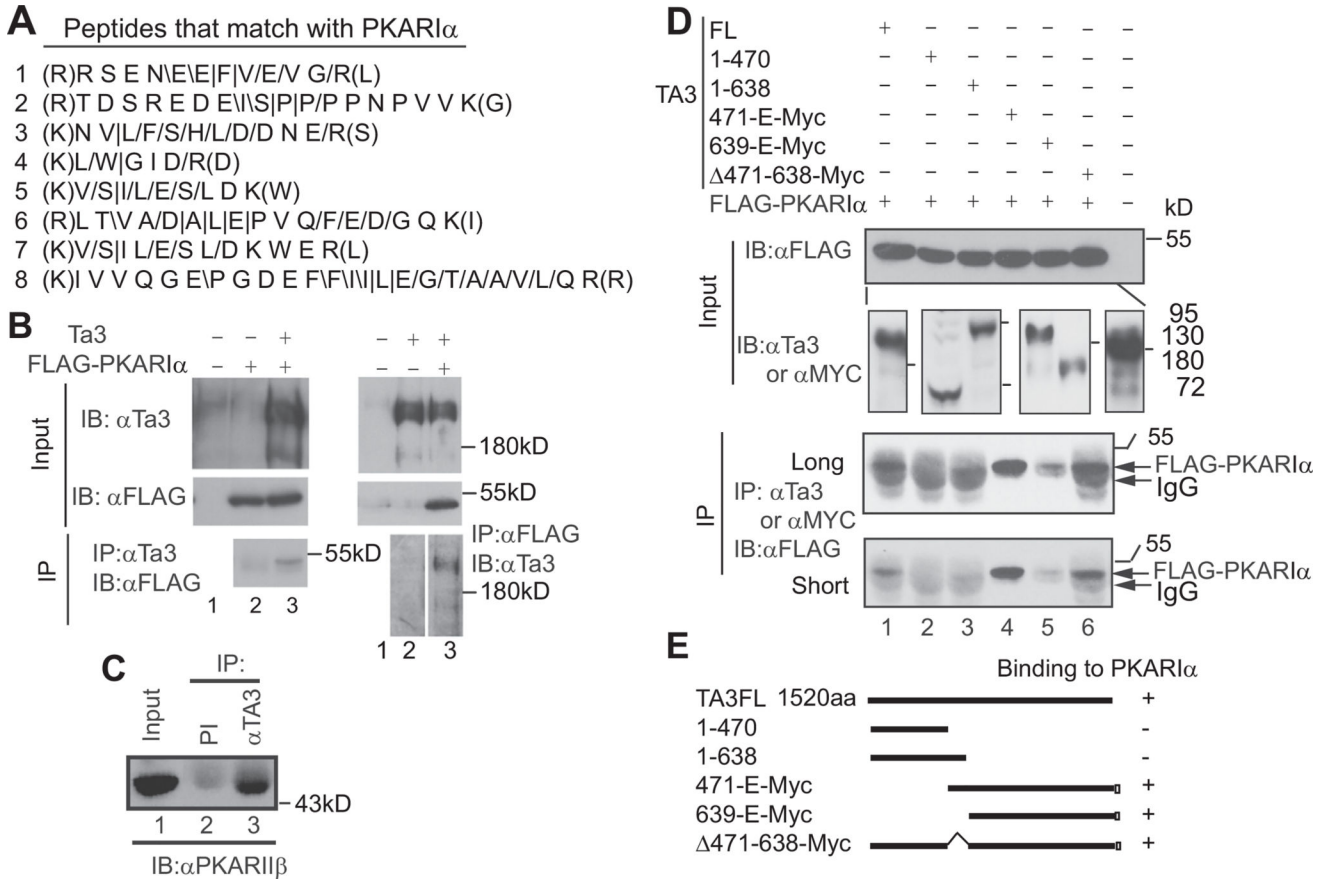

Fig. 4.

The Ta3 C-terminus interacts with PKA regulatory subunits. (**A**) The peptides obtained from mass spectrometry match with PKARIα. /, /, and | are referred to as *y*-ions, *b*-ions, and both, respectively. They were detected in the tandem mass spectrometry analysis of the peptides. (**B**) Coimmunoprecipitation showing that Ta3 interacts with FLAG-PKARIα in transfected HEK293 cells. (**C**) Coimmunoprecipitation showing that endogenous Ta3 interacts with PKARIIβ. (**D**) Coimmunoprecipitation showing that the C-terminal region of Ta3 interacts with PKARIα. Subpanels in the second panel from the top are from different immunoblots. The molecular weight markers correspond to the lines in each subpanel in the order. Two lower panels are the same with different exposure time. (**E**) Diagrams showing constructs and summary in D. IP, immunoprecipitation; IB, immunoblot; PI, preimmune serum.

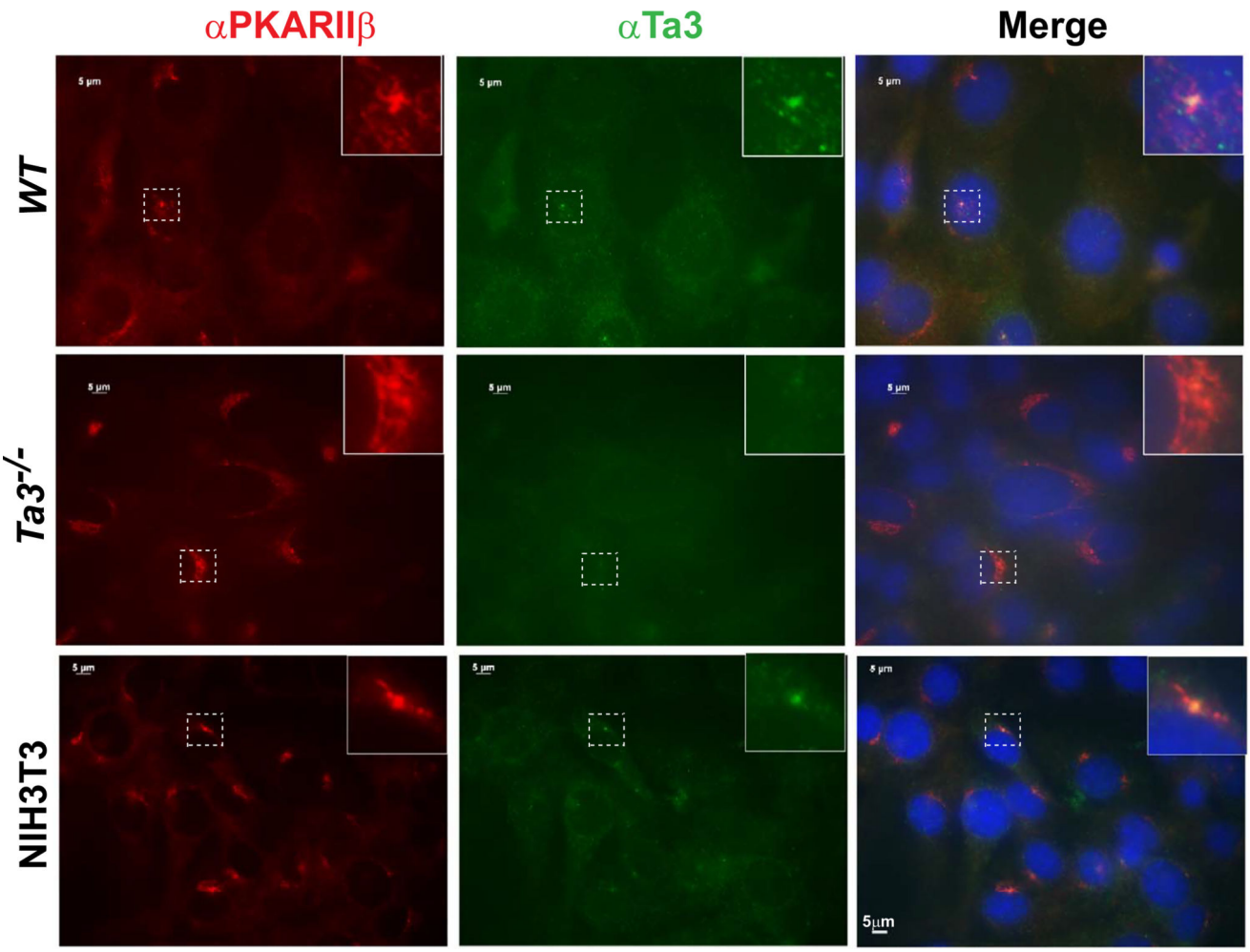

Fig. 5.

Ta3 and PKARIIβ colocalize at centrioles in the cell. Wild type (WT) and *Ta3* mutant MEFs and NIH3T3 cells were stained for PKARIIβ, Ta3, and nuclei (DAPI, blue). Ta3 staining is specific, as no signals were detected in *Ta3* mutant cells. Insets are the enlargement of the framed areas with dash lines.

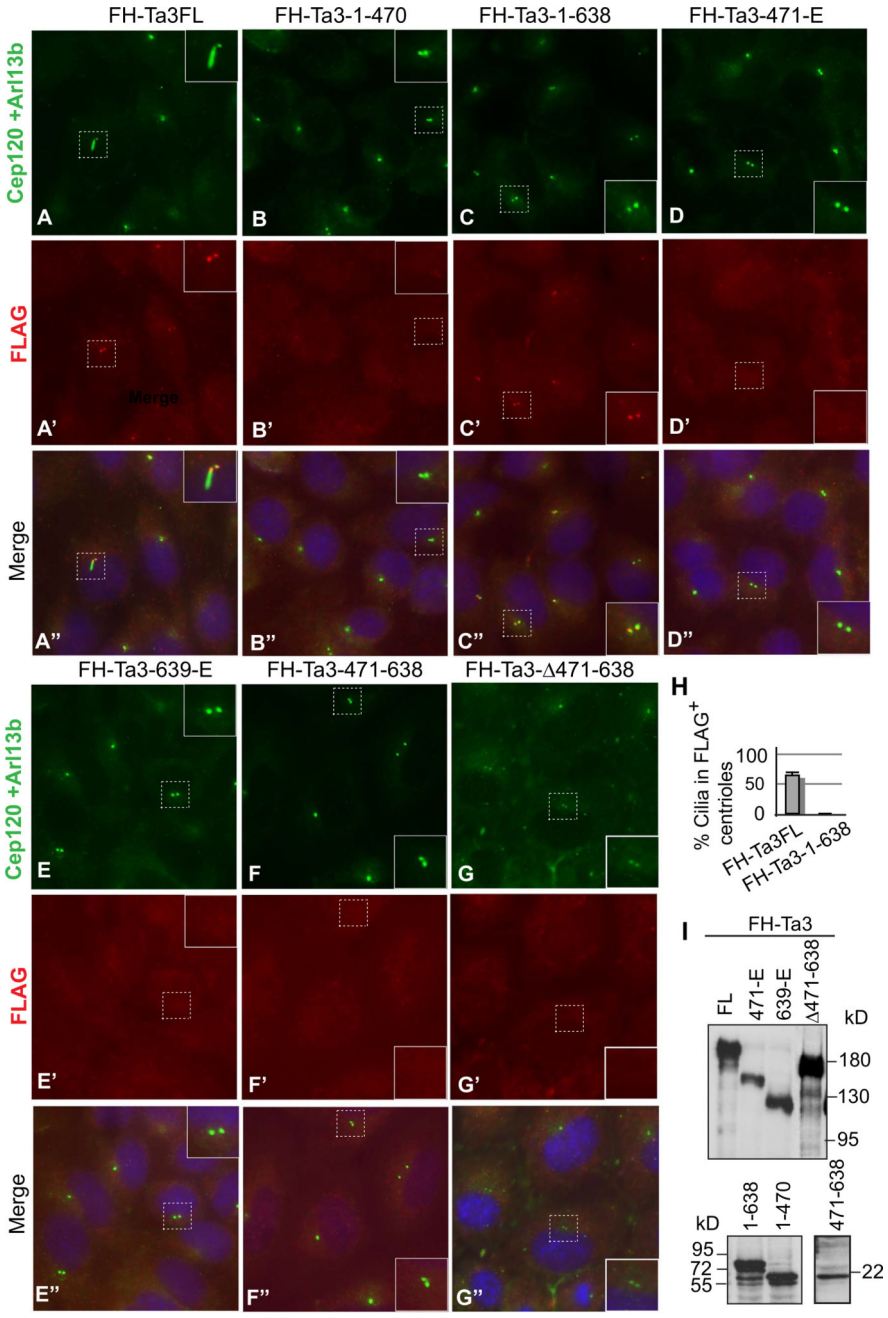

Fig. 6.

Expression of Ta3FL, but not Ta3 mutants, rescues ciliogenesis in *Ta3* mutant cells. (**A–G"**) *Ta3* mutant MEFs were transduced with the retrovirus carrying the constructs indicated above the panels. Following serum starvation, the cells were stained with FLAG, Cep120, and Arl13b antibodies and counterstained with DAPI for nuclei. FLAG labels Ta3 and mutants. Cep120 marks centrioles, and Arl13b is a cilia marker. Insets are enlargement of the framed areas with dash lines. Note that although both FH-Ta3FL and FH-Ta3-1–638 localize at centrioles, only FH-Ta3FL expression rescues cilia formation. (**H**) A graph showing that the percent cells that are FLAG-staining positive at centrioles form cilia. Two-

tailed Student *t*-test p-value = 0.0001 (n=72). (**I**) Immunoblots showing the expression of Ta3 and mutant proteins.

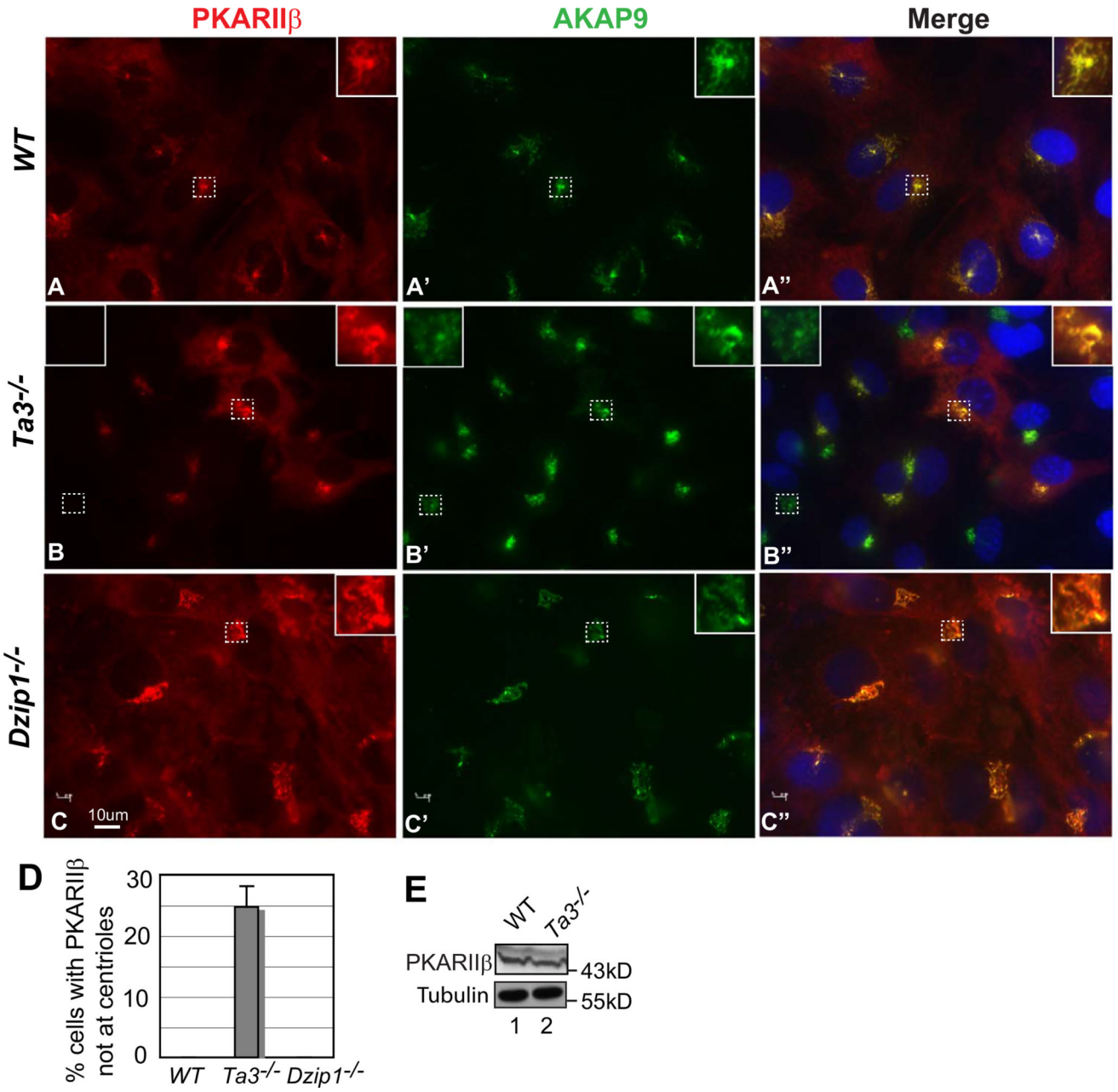

Fig. 7.

PKARIIβ is not colocalized with AKAP9 at centrosome in some *Ta3* mutant cells. (**A**–**C**) WT, *Ta3*, and *Dzip1* mutant MEFs were stained for PKARIIβ, AKAP9, and nuclei (DAPI, blue). Insets are the enlargement of the framed areas with dash lines. Insets in the right show colocalization, whereas an inset in the left shows a lack of colocalization. (**D**) The percentage of *Ta3* mutant cells that lack PKARIIβ staining at centrioles. The graph was derived from three independent experiments. Note that PKARIIβ mislocalization is only detected in *Ta3* but not *Dzip1* mutant cells. P-value = 0.0002 ($n \geq 60$). (**E**) Immunoblot showing the similar PKARIIβ levels in wt and *Ta3* mutant cells.